Application of PFC^{3D} to simulate a planetary ball mill

L. Guzman[1], Y. Chen[1*], S. Potter[2], M.R. Khan[1]

(1.Department of Biosystems Engineering, University of Manitoba, Winnipeg, MB, Canada;
2.Composites Innovation Centre, Winnipeg, MB, Canada)

Abstract: Planetary ball mill is a versatile machine which has been used for grinding different types of materials for size reduction and lately for hemp decortication. PFC^{3D}, software employing the discrete element method (DEM), was used to simulate the power and energy requirement of grinding hemp for fibre using a planetary ball mill. The simulation was facilitated through a series of hemp grinding tests using the planetary ball mill to examine the power draw of the mill. The test results identified that grinding speed had a significant effect on the power draw of the mill. The power draw data were used to calibrate the discrete element parameters for different grinding speeds. Using the calibrated parameters, one was able to predict the kinetic energy and friction power loss of the ball mill. The average value of kinetic energy predicted, for grinding speeds of 200 – 500 r/min, ranged between 0.01 and 0.07 J per grinding ball. The prediction showed that frictional power losses dispersed approximately 10% of the total power requirement of the ball mill. Overall, the simulation using PFC3Dimproved understanding about the dynamics of the grinding balls within a planetary ball mill as well as the energy available for transfer in collisions between the grinding balls and hemp material.

Keywords: PFC^{3D}, Discrete element model (DEM), hemp, planetary ball mill, power, energy, kinetic, friction

Citation: Guzman,L.,Y. Chen, S. Potter, and M.R. Khan. 2015. Application of PFC3D to simulate a planetary ball mill. Agric Eng Int: CIGR Journal, 17(4):235-246.

1 Introduction

Planetary ball mills are well suited for laboratory-scale processing of materials in diverse industries (Rosenkranz et al., 2011). A future objective of industry is to develop large-scale units for industrial manufacturing purposes. Overall, ball mills were able to defibrillate fibrous materials as well as improve fibre fineness by applying impact and shear forces (Prasad et al., 2005). Previous studies by our research group have demonstrated promising potential of ball milling for hemp (*Cannabis sativa Linnaeus*) decortication (Baker et al., 2010) and for hemp fibre refining (Khan et al., 2009). Decortication is a mechanical process of extracting raw hemp fibres, which is an energy intensive process because hemp plants possess a high percentage of cellulose and lignin. Commonly used decortication equipment for hemp includes hammer mills, cutter heads, and roll crushers. Each piece of decortication equipment operates under different principles involving the application of forces to the hemp stalk and obtaining the fibre (Fürll and Hempel, 2000; Gratton and Chen, 2004). All of these machines have multiple rotating parts, such as shafts and bearings, which are in contact with hemp, causing hemp fibre wrapping around these rotating parts (Dietz, 1999; Hobson et al., 2001). Hence, an operational limitation of these machines is the need for frequent stops to remove wrapped fibres and prevent any further damage to the machines. Ball mills are alternative machines for hemp decortications. The main advantage of using ball mills is that fibres are not in contact with any rotating machine parts. Hence, fibre wrapping problems are no longer a concern.

The focus of this study was on the dynamic behaviours of a planetary ball mill in the context of hemp decortication. The working principle of a planetary ball mill is based on the movement of a grinding bowl, filled with grinding balls. The grinding balls are subjected to

Received date: 2014-07-28 Accepted date:2015-09-20
***Corresponding author: Ying Chen,** Department of Biosystems Engineering, University of Manitoba, Winnipeg, Manitoba R3T 5V6, Canada. Tel.: 1 204 474 6292. fax: 1 204 474 7512. E-mail: ying_chen@umanitoba.ca.

superimposed rotational movements. The difference in speeds between the grinding balls and grinding bowl produces an interaction between frictional and impact forces, which releases high dynamic energy. Inside a planetary ball mill, multiple collision events transfer impact energy from the grinding balls to the material (e.g. hemp sample) (Lynch and Chester, 2005). The energy available for all collision events is provided by the movement of the grinding bowl, which is driven by an electric motor. Hence, there is a direct relationship between the total power draw of the mill and impact energy of the grinding balls. To design efficient and effective ball mills, research is required to provide information about energy transfer mechanisms acting within the planetary ball mill. The information includes power requirement, kinetic energy, and frictional power loses. Since direct observation by means of on-line sensors is impractical, and dynamic behaviours of grounding balls and their interactions with material are very complex and difficult to measure, the best option is numerical simulation (Mishra, 2003a).

One of the most effective methods of simulating behaviours of individual particles (e.g. grinding balls) is using the discrete element method (DEM). The DEM is a time-stepping algorithm that requires three main elements: the repeated application of Newton's second law of motion to each particle (grinding ball) inside the considered system (grinding bowl); a force–displacement law to each contact; and a constant update of particle (grinding ball) and wall (grinding bowl) positions. The DEM has been successful at approximating ball milling internal behaviour and motion patterns. Radziszewski (2002) modelled media wear mechanisms of a mill using the DEM. The model was calibrated and validated with lab tests of ore-metal. That study also listed other studies using the DEM to describe the dynamics inside mills. Cleary and Hoyer (2000) simulated the charge motion of a centrifugal mill in an application of grinding quartz using steel balls. The most significant affecting factor reported was the mill operational speed (rpm).Planetary ball mills have been also modelled using the DEM. The motion of steel balls was affected by the type of feed and the friction of the media (Rosenkranz et al., 2011). Sato et al. (2010) tried to relate wear to the impact energy of steel balls of a planetary ball mill. They found that wear rate increased with the increase of mill operational speed, ball diameter, and ball-filling ratio.

One of common DEM softwars, Particle Flow Code in Three Dimension (PFC^{3D}), has several features which are suitable for simulation of a planetary ball mill. Using PFC^{3D}, moving balls in a mill can be described with translational and rotational motions. It also takes frictional force into consideration between the contacts of balls. Several dynamic attributes of balls, such as kinetic energy and friction energy, can be monitored while the ball mill is in operation.

In summary, little work has been done on planetary mills with non-steel material as media and using PFC^{3D}as the modelling tool. The objectives of this study were to: 1) apply $PFC^{3D}$to simulate a planetary ball mill; 2) calibrate the PFC^{3D} parameters with measurements from hemp decortication; and 3) predict dynamic behaviours of grinding balls inside the mill.

2 Methodology

2.1 Description of the planetary ball mill

A planetary ball mill (Fritsch Pulverisette 6 classic line, Idar-Oberstein, Germany) was used in this study. The machine consisted of a cylindrical grinding bowl with an inner diameter of 74.5 mm and a height of 86.7 mm (Figure 1a). The effective volume of the bowl was 250 ml. The grinding media consisted of 15 spherical balls (Figure 1b) with a 20-mm diameter. The balls were made of agate with a density of 2650 kg/m^3. The inside of the bowl had an agate liner. Thus, the interaction between the bowl and balls was agate to agate. The bowl was fixed on a support disc (Figure 1c) and the distance between the axle of the bowl and the axle of the support disc was 62.5 mm. The mill was powered by a 1.1 kW electric motor. The bowl rotated about its own axis in one direction and

also rotated with the support disc in the opposite direction. The relative speed ratio of the bowl to the supporting disc was 1.82. For every full rotation of the disc, the grinding bowl rotates 1.82 revolutions about its own centre in the opposite direction.

Figure 1 Principal components of a planetary ball mill: (a) grinding bowl; (b) grinding balls; (c) relative position of the grinding bowl on the supporting disc

2.2 Simulation

2.2.1 Model of the planetary ball mill

All the dimensions and properties of the ball mill within the model were equivalent to those of the aforementioned planetary ball mill. The PFC^{3D} version 4.00 was used to develop the model of the planetary ball mill. The main component of the model was the assembly of grinding balls which were represented by spherical particles (Figure 2). The constitutive laws for the contact between particles were described by the Stiffness and Slip Models implemented in PFC^{3D}. These Models provide an elastic relation between the contact force and the displacement of particles, and allow two contacting particles to slip relative to each other, introducing a friction force between the particles.Rosenkranz et al. (2011) reported some significant effects of rolling friction of particle, whereas Cleary and Hoyer (2000) reported mixed results about the effects of rolling friction, depending on the mill fill level. It is advised that rolling friction was not considered in the model of this study.

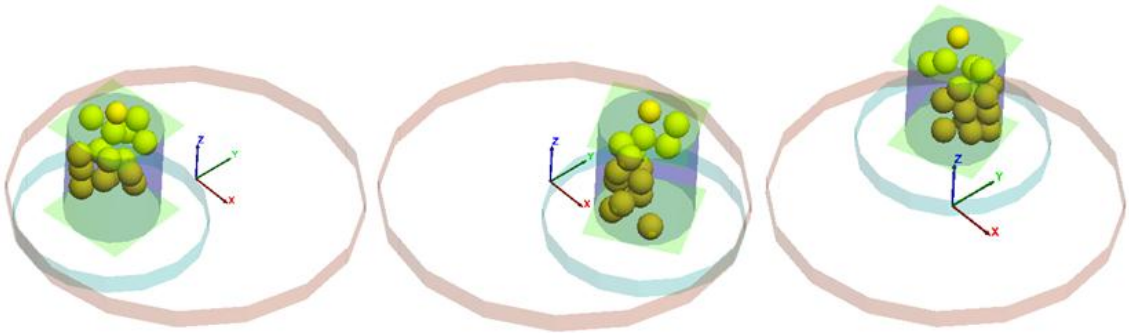

Figure 2 Screenshots of the model planetary ball mill at different simulation time steps

Fifteen balls were enclosed inside a bowl which was constructed using a cylindrical wall as the body of the bowl and two flat square walls as the bottom and top covers of the bowl. The largest disc functions as the

supporting disc. The medium-sized disc is the grinding bowl support, and it was used to ensure that the distance between the centre of the bowl and the centre of the support disc was constant at all times. At the commencement of the simulation, it was assumed that the grinding balls were settled at the bottom of the bowl. The grinding balls were generated inside the bowl and the model was operated in a stationary state to allow the balls to settle at the bottom of the bowl due to the force of gravity. Before running the simulations, a detailed examination of the location of the grinding bowl was performed to ensure the right relative motion and position between the grinding bowl and supporting disc. This was done through monitoring the position of the grinding bowl with a tracking particle following the same motion pattern as the grinding bowl support. The tracking particle was located in the centre of the grinding bowl and it was positioned in such a way that it would not interact with the grinding balls inside the grinding bowl.

2.2.2 Motion generation

Figure 3 shows a simplified diagram of the relative motion of the grinding bowl with respect to the supporting disc. The rotational speed of the supporting disc was an adjustable variable in the simulation and was assigned values corresponding to the tests. As described earlier, the angular velocity of the grinding bowl about its own centre was given by Equation (1):

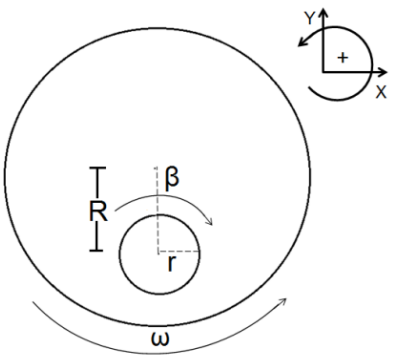

Figure 3 Motion diagram of the planetary ball mill (R = distance from the centre of the supporting disc to the centre of the grinding bowl; r = radius of grinding bowl; ω = angular velocity of supporting disc; β = angular velocity of the grinding bowl)

$$\beta = -1.82\,\omega \qquad (1)$$

where

β = angular velocity of the grinding bowl, rad/s;

ω = constant angular velocity of the supporting disc, rad/s.

The motion produced by the supporting disc was modelled as a function of ω and time. The absolute linear velocity of the centre of the grinding bowl with respect to the centre of the supporting disc was given by Equation (2):

$$V = R\omega \qquad (2)$$

where

V = absolute linear velocity of the centre of the grinding bowl, m/s;

R = distance from the centre of the grinding bowl to the centre of the supporting disc, m.

The function for circular displacement of the grinding bowl about the centre of the supporting disc was categorized as two-dimensional motion parallel to the plane of the supporting disc. The function for circular displacement was obtained by breaking the absolute linear velocity into two vector components, V_x and V_y. The magnitude of these vector components was given as a function of the time required to complete one full revolution with boundary conditions as illustrated in Figure 4.

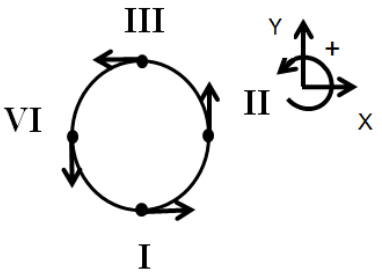

	I	II	III	IV
V_x	V	0	-V	0
V_y	0	V	0	-V

Figure 4 Boundary conditions for vector components of the linear velocity

The Equation (3a) and Equation (3b) for the vector components of the absolute displacement velocity were derived as:

$$V_x = \cos\left(\frac{\pi}{2t_{\frac{1}{4}}}t\right)V \qquad (3.a)$$

$$V_y = \sin\left(\frac{\pi}{2t_{\frac{1}{4}}}t\right)V \qquad (3.b)$$

where

$t_{1/4}$= the time required to complete one quarter of a revolution, s;

t = the total accumulated time of the model, s.

The value of $t_{1/4}$ was fixed depending on the magnitude of the rotational speed of the supporting disc. The variable t started at zero and increased with each time step in the same units as $t_{1/4}$. The value of $t_{1/4}$ was derived directly from the number of revolutions per minute as Equation (4):

$$t_{1/4} = \frac{15}{n} \qquad (4)$$

where

n = number of revolutions per minute, r/min.

Application of the previously described boundary conditions produced the desired motion within the model. The proposed system of equations worked for any assigned speed, while maintaining the same geometrical relationships found in the planetary ball mill. Figure 5 shows the displacement velocities of the centre of the grinding bowl with respect to the centre of the disc. Simultaneously, the grinding bowl constantly rotated about its own centre at an angular velocity equivalent to β.

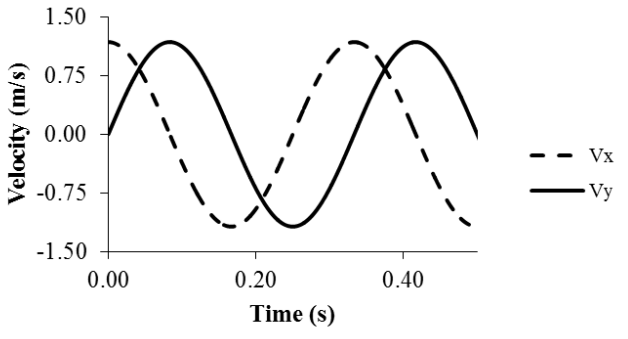

Figure 5 Change in velocity components over time at 200 r/min

2.2.3 Model parameters

The integration of DE equations required parameters which describe the contact nature between balls and bowl. The application of linear contact models was discussed in the work of Mishra (2003b). The linear model is defined by the normal and shear stiffness, K_n and K_s, of the two contacting entities (ball-to-ball and ball-to-wall). Stiffness had some effects on the internal dynamics of mill (Cleary and Hoyer, 2000). In this study, this parameter was determined from the Young's modulus of the material (Cundall and Strack, 1982; Chang et al., 2003) using the following Equation (5) (Itasca, 2012):

$$K_n = 4R_p\bar{E} \qquad (5)$$

where

K_n= the normal stiffness, N/m;

R_p= the ball radii, m;

E = the apparent young's modulus, Pa.

The grinding balls and the walls within the model were assigned contact properties that were equivalent to Agate stones, with a density of 2650 kg/m^3 and a modulus of elasticity of 70 GPa (Fossen, 2010). Application of the relationship in Equation (5) resulted in a normal stiffness, K_n, value of 2.8x10^9 N/m. The shear stiffness, K_s, was assigned the same value as the normal stiffness as in many other studies (e.g. McDowell and Harireche, 2002; Asaf et al., 2007). A low value was taken for the friction coefficient of the balls, considering their polished surfaces. The values of all model parameters are summarized in Table 1.

Table 1 DEM parameters applied to simulation

Model parameter	Value
Ball density, kg/m^3	2650
Ball diameter, mm	20
Number of balls	15
Normal and shear stiffness, N/m	2.8x10^9
Friction coefficient	0.3

2.2.4 Damping coefficients

In DE models, energy supplied to the particles needs dissipation with damping mechanisms to arrive to a steady state solution (Itasca, 2012). The PFC^{3D} code is able to dissipate kinetic energy with two types of damping, local and viscous damping. Local damping (L_d)

applies a damping force to each ball, while viscous damping applies the damping force to each contact (ball-ball or ball-wall).Viscous damping has two damping components, normal (V_{dn}) and shear (V_{ds}). As a general rule of thumb, local damping is most appropriate for compact assemblies while viscous damping is preferred for situations involving free flight of particles or impacts between particles. The planetary ball mill was subject to both scenarios because it behaved as a compact assembly at low grinding speeds but particles took flight and collided at higher grinding speeds. The combination of these two types of damping would provide the most accurate physical representation of the ball assembly, and they were calibrated.

2.3 Calibration of the damping coefficients

The damping coefficients (L_d, V_{dn}, and V_{ds}) were calibrated using measurements of the ball mill power from tests. The tests and calibration method are described in the following sections.

2.3.1 Measurements of power requirement of the ball mill

To calibrate the model, data on the power requirement of the mill were collected in tests of hemp grinding. Hemp samples (variety: USO 31) were stored to air dry to a moisture content of approximately 10%. Before being ground, hemp samples were cut into 40-mm stalk segments so that they could fit into the grinding bowl. The grinding bowl was filled with an approximately six grams based on the ball mill feeding capacity. The magnitude of the power requirement for grinding was expected to be affected mainly by the mill speed. A range of different grinding speeds was selected: 200, 300, 400, and 500 r/min according to the operational specifications of the mill. Power requirement may also change over time while a hemp sample is being ground, as the hemp particle size changes over time. Therefore, grind tests were performed for three grinding durations: 3, 5, and 8 min at each grinding speed. The power draw in the grinding process was measured with a watt-hour meter directly connected to the ball mill. Before each test, the power consumption without hemp was recorded for 5 min. Comparison of the average power draws between the conditions with and without samples served as a means to determine the net power draw for hemp grinding.

2.3.2 Model prediction of power

The ball mill model was run at the default time step of PFC^{3D}to predict the power required for moving the grinding balls inside the bowl. This power is equivalent to the total accumulated work of the walls (i.e. the inside of the grinding bowl) on the assembly of balls. The PFC^{3D} is able to monitor this work which is defined as Equation (6) (Itasca, 2012):

$$E_w = \sum_{Nw}(F_i \Delta U_i + M_i \Delta \theta_i) \quad (6)$$

where

E_w = the total accumulated work of the wall;

N_w = the number of walls (one cylindrical wall and two flat walls in this case);

F_i and M_i = the resultant force and moment acting on the walls, respectively;

U_i and θ_i = the applied displacement and rotation, respectively.

Under the assumption that all the energy provided to the systems originated from this source, the power was calculated through the magnitude of E_w divided by the total accumulated time. The magnitude of E_w was positive or negative, with the convention that work of the walls on the particles is positive. Calibrations of damping coefficients were performed through comparisons of the powers measured and simulated. The calibrated damping confidents were those values which resulted in the best match between measurements and simulations.

3 Results and discussion

3.1 Tests and calibration results

3.1.1 Measured power requirement

The difference between power draw measurements with and without hemp samples, was used to calculate the net power draw required to grind the samples. The average values of net power draw ranged between 0 and 3

W, which was only approximately 1%-5% of the total power draw measured. A paired t-test, with a 5% level of significance, showed that the differences in draw power were insignificant between the conditions with and without hemp sample in the bowl. In addition, the net power data had no particular trends, in terms of effects of grinding speed and duration. Although the hemp sample occupied a significant volume inside the grinding bowl, it did not affect the power required to operate the mill. A possible explanation is that the hemp sample possessed a relatively small mass of grinding balls. The tests demonstrated that grinding media (balls) and its dynamics were the major factors affecting the power draw of ball milling.

Given the insignificant differences between tests with hemp and without hemp, the total power data pooled from the tests with hemp and without hemp were used to examine effects of grinding speed. The results showed that milling at larger rotational speeds required increasing amounts of input power (Figure 6a and Figure 6b). The relationship between the power draw and rotational speed could be described as a linear relationship with a coefficient of determination of 0.99. The results showed that the power draw did not vary with the grinding duration (data not shown). For example, at 400 r/min, power draw was determined as 151 ± 6, 152 ± 7, and 153 ± 9 W for 3, 5, and 8 min respectively.

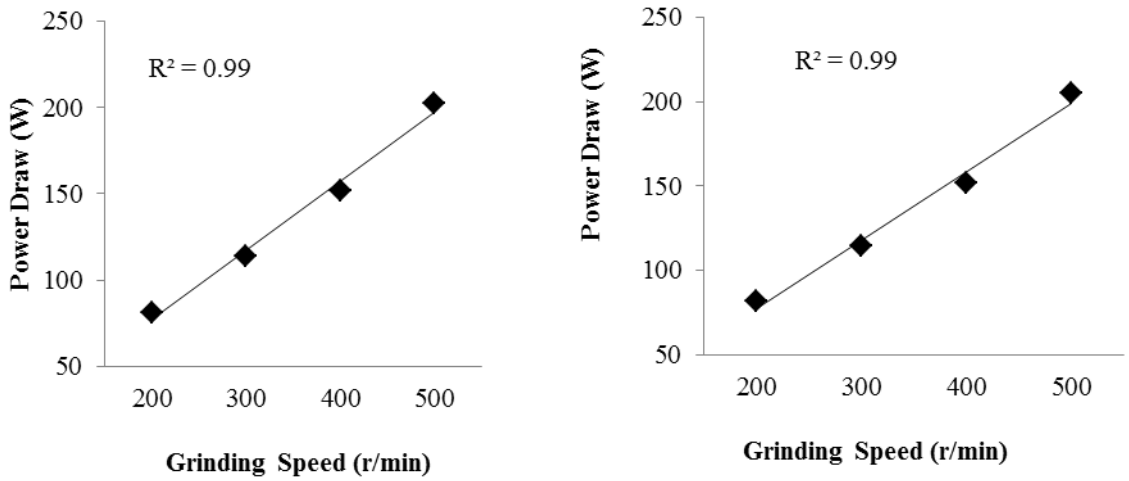

(a) (b)

Figure 6 Variations of power draw of the planetary ball mill with grinding speed: (a) with hemp sample; (b) without hemp sample

3.1.2 Effects of damping coefficients on the power requirement

Simulations demonstrated that as the damping coefficients were adjusted, dissipation of more energy due to damping would cause lower magnitudes of the power predicted by the model. An example of this type of behaviour is present in Figure 7, in which every parameter remains constant with the exception of two damping coefficients. It was clear that the damping coefficients significantly affect the model outputs both over time and in magnitude. Dynamic behaviours of the ball assembly were very sensitive to the input viscous damping coefficients.

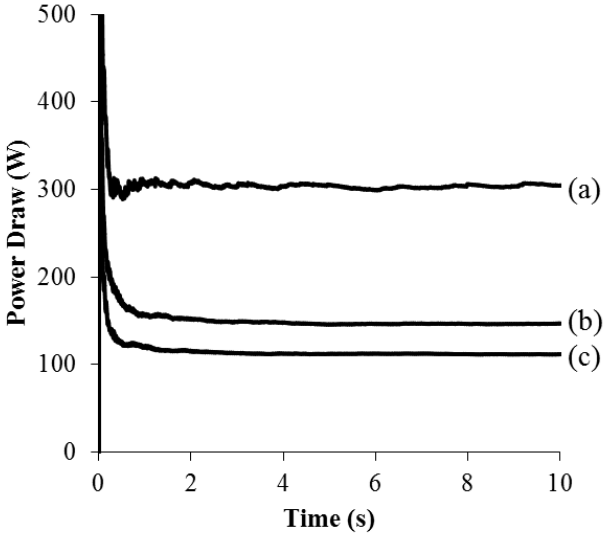

Figure 7 Effect of damping coefficient on power draw at 400 rpm; L_d=0.4: (a) V_{dn}= V_{ds}=0; (b) V_{dn}= V_{ds}=0.3; (c) V_{dn}=V_{ds}=0.6 (L_d=local damping coefficient; V_{dn} andV_{ds}=viscous normal and shear damping coefficients respectively)

3.1.3 Power comparisons between simulations and measurements

The test results demonstrated that the addition of hemp material and grinding duration did not significantly affect the power draw. This information provided the base for simplifying the model without involving hemp particles in the model, which allowed for a representative simulation of the planetary ball mill. The measured power draw was the total energy introduced into the planetary ball mill from the electricity source. The difference between the measured power draw and the simulated power was that the measured power included the mechanical loss in the process of transmitting electricity energy to the ball assembly. The mechanical loss was assumed as 10% of the total power draw (Wills, 1979). Thus, the values of the measured power draw were reduced by 10% before being compared with the powers predicted by the model.

The power was simulated for multiple combinations of L_d, V_{dn}, and V_{ds} at different grinding speeds (200, 300, 400, and 500 r/min). The results showed that changes in L_d had little influence in power after the grinding balls engaged in free flight, whereas changes in V_{dn} and V_{ds} had significant effects in the power. For simplicity, values of L_d were kept constant for the different grinding speeds and values of V_{dn} and V_{ds} were kept the same for each speed. Results demonstrated that there was not a single value of V_{dn} and V_{ds} that would accurately approximate the power draws measured for all grinding speeds. For example, with a value of V_{dn} and V_{ds}, the predicted value of power for the 200 rpm would be comparable to the measurements, but that for the 300 rpm would have a relative error of over 40% when compared to the measurement. These results indicated that the V_{dn} and V_{ds} were grinding speed dependent. Hence, a specific value of V_{dn} and V_{ds} was required to be calibrated for each grinding speed.

In calibrating the damping coefficients for different grinding speeds, it was found that a constant value (0.4) was an adequate L_d for all speeds. With this constant L_d, the input V_{dn} and V_{ds} were being adjusted during the simulation until the predicted power best matching the measured one. The best match was considered as the least relative error between the predicted and measured powers. Table 2 lists the calibrated results and the least relative errors obtained. The calibrated values of V_{dn} and V_{ds} were increased as the grinding speed increased, which represented the slowing down of grinding balls. The average relative errors for the speeds of 200, 300, and 400 rpm were all below 10%, which indicated that the model was able to adequately approximate the power. However, the relative error for the 500 rpm was quite high (28.2%).

Table 2Calibrated damping coefficients for different mill speeds

Speed, r/min	Damping Coefficient			Power, Watts		
	L_d	V_{dn}	V_{ds}	Model	Test	Relative Error, %
200	0.4	0	0	81.6	81.4	0.31
300	0.4	0.3	0.3	102	114	9.96
400	0.4	0.6	0.6	147	152	3.19
500	0.4	1.2	1.2	264	204	28.2

3.2 Simulations of dynamic behaviours of the planetary ball mill

The calibrated model was used to simulate the kinetic energy and friction loss of the ball assembly. To better understand these, motion patterns of the balls were also visually examined. All simulations were performed under different grinding speeds using the calibrated damping coefficients listed in Table 2.

3.2.1 Motion pattern of the balls

Figure 8 provides an example of monitoring grinding balls to determine their locations after one full revolution. The grinding balls followed a cascading type of motion for the proposed range of grinding speeds. The grinding balls were "flying" towards the opposite end of the cylinder wall. Movement of the grinding balls within the ball mill led to collisions, which became the main mechanism transferring energy from the grinding balls to the hemp sample.

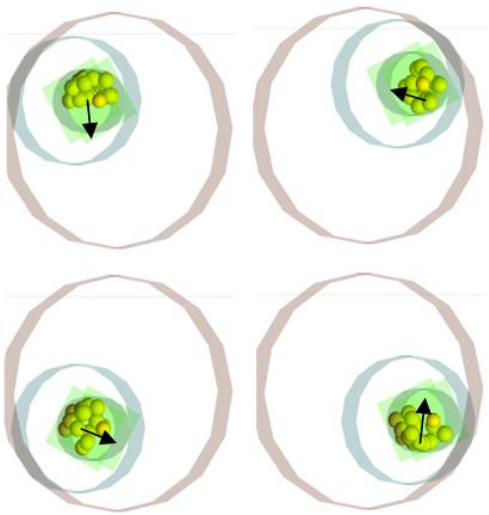

Figure 8 Screenshot of grinding ball motion pattern after one full revolution of the grinding bowl

The monitoring of the velocity distribution within grinding balls helps supplement grinding ball position information. The proposed model was able to record the translational velocity distribution at different grinding speeds. The velocity distribution (Figure 9) indicates that grinding balls adjacent to the bowl wall have a different translational velocity than those closer to the centre of the grinding bowl. The differences in translational velocities were in the order of 0.5 m/s, which support the argument for calculating the average kinetic energy of each ball as the average kinetic energy within the model.

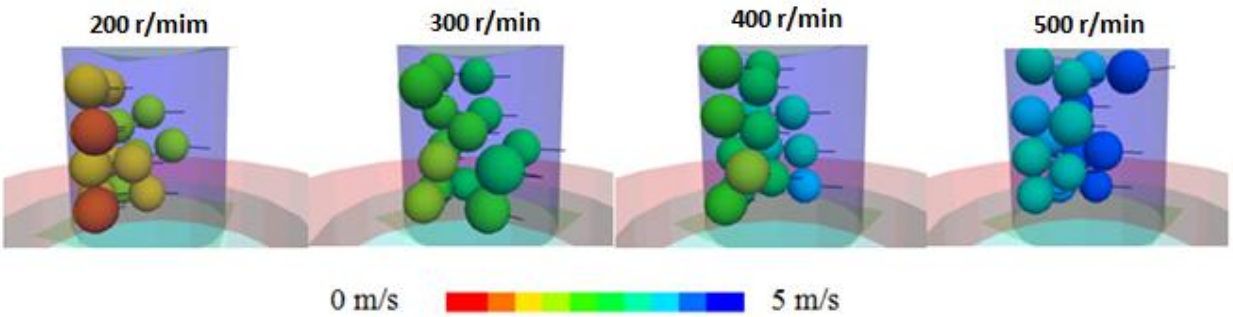

Figure 9 Velocity distribution of grinding balls at different grinding speeds

Through enhanced understanding of motion patterns, the DEM enabled future study of design factors such as the operational grinding speed, sizes of the grinding balls and bowl, friction coefficients, and the ratio of material to bowl volume. These design factors have a direct effect in the effectiveness and location of the grinding areas where high impact forces decorticate the hemp sample.

3.2.2 Kinetic energy of the balls

Previous studies (Abdellaoui and Gaffet, 1995; Magini et al., 1996; Iasonna and Magini, 1996) determined collision energy by linking it directly to the kinetic energy of each individual grinding ball. The collision energy in the planetary ball mill was assumed equivalent to the total kinetic energy of the balls' motion. The proposed model was able to determine the total kinetic energy of all particles accounting for both translational and rotational motion as Equation (7) (Itasca, 2012):

$$E_k = \frac{1}{2}\sum_{Nb}(m_i V_i^2 + I_i\omega_i \cdot \omega_i) \quad (7)$$

where

E_k = total kinetic energy;

N_b, m_i, I_i, V_i and ω_i= the number of balls, inertial mass, inertia tensor, and translational and rotational velocities of ball i, respectively.

The average kinetic energy provides information about the amount of energy available for transfer from the grinding balls into the hemp stems. Average kinetic energy was approximated for each ball from the division of the total kinetic energy by the number of grinding balls present in the model. The average magnitude of the modelled kinetic energy, for each given grinding speed, consisted of slight diversions in magnitude about an average value. An example of the kinetic energy output from the model is shown in Figure 10, which includes the range of values of the total kinetic energy including all grinding balls at a grinding speed of 200 r/min for 10 s.

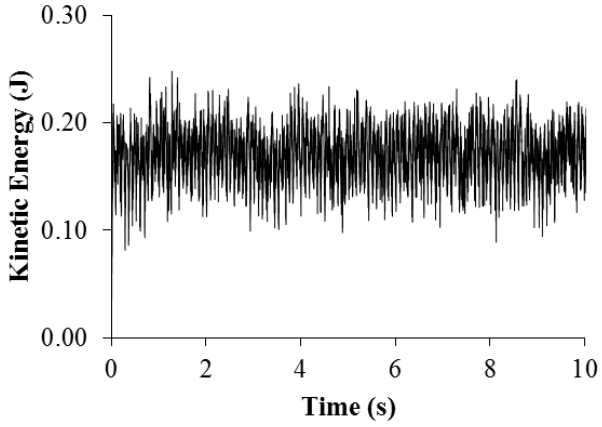

Figure 10 Simulated total kinetic energy predicted by the model for the 200 r/min grinding speed

Results of the average kinetic energy per ball obtained from the model were plotted in Figure 11. The order of magnitude of the predicted kinetic energy was in accordance with studies performed by Magini et al. (1996), who established that the collision energy of individual balls was in the order of 10^{-2} J per collision. The best fit curve of the data was found to follow a power relation with a coefficient of determination of 0.98. The predicted kinetic energy provided information about energy transferred from the grinding balls into the hemp sample during milling.

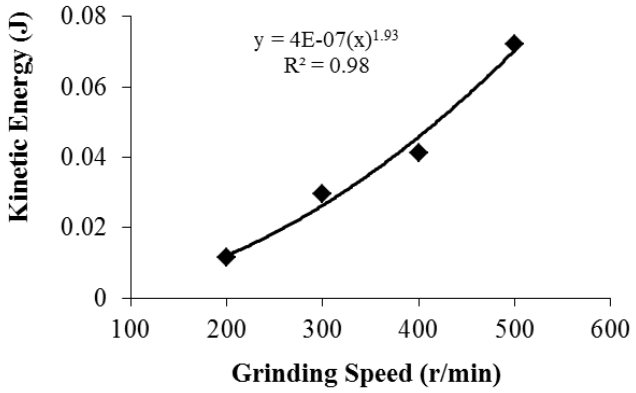

Figure 11 Simulated average kinetic energy per ball at different grinding speeds

3.2.3 Frictional power losses

A portion of the power introduced into the system was dispersed as frictional energy. Within the proposed

model, the total accumulated frictional energy loses was defined (Itasca, 2012) as Equation (8):

$$E_f = \sum_{Nc}(F_{is}\Delta U_{is}) \quad (8)$$

where

E_f = total accumulated frictional energy loss;

Nc = the number of contacts;

F_{is} and ΔU_{is}= the average shear force and the increment of slip displacement respectively.

The parameter E_f represents the magnitude of the total accumulated energy dissipated through frictional sliding at all contacts. The total friction power losses were calculated from dividing the total energy dissipated through friction with the total accumulated time. Figure 12 shows a typical curve of friction loss over time.

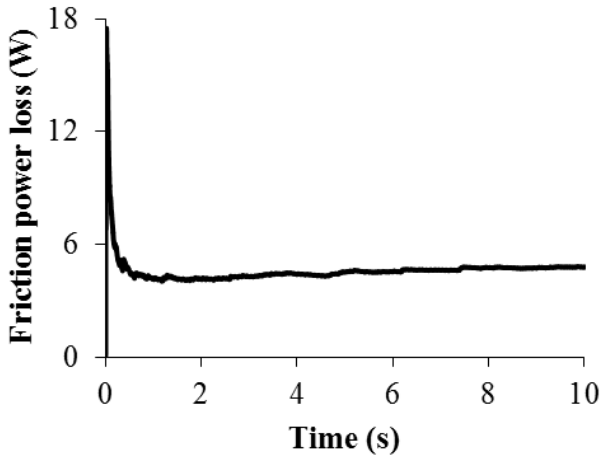

Figure 12 Simulated friction power losses at 200 r/min

The magnitude of the frictional power losses increased at larger grinding speeds (Figure 13). However, frictional power losses represented only a small percentage of the total power. The energy dispersed through friction at 200, 300, 400, and 500 rpm accounted for 5.7%, 11%, 11%, and 13% of the total power respectively. In average, it was determined that approximately 10% of power was dispersed as frictional energy. After frictional losses, the remaining applied energy is mostly in the form of kinetic energy driving high energy impacts during the milling process.

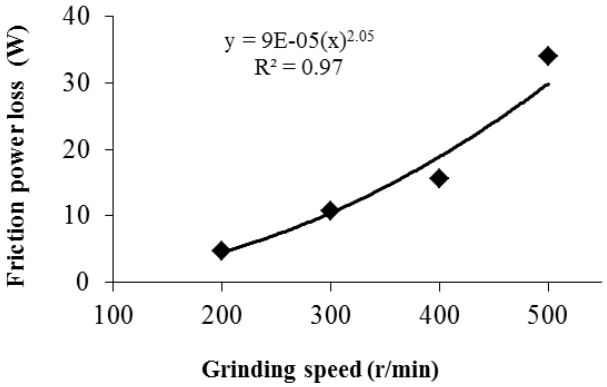

Figure 13 Friction power losses at different grinding speeds

Although further experiments are required to determine the applicability of current model parameters to different types of milling arrangements, the PFC^{3D} could potentially evaluate the effect of various conditions through changing the variables such as grinding media, grinding speed, and mill dimension. Hence, the proposed model improves its capacity to recreate and understand the dynamics inside a planetary ball mill.

4 Conclusions

The planetary ball mill was successfully modelled using a PFC^{3D} with appropriate geometrical relationship of the motion in the grinding bowl. Test results showed that the energy consumption of milling hemp was attributable mainly to the grinding media, not the hemp being ground.Based on the test results, the model was simplified without considering effects of hemp material.It was found that viscous damping coefficients were the most crucial model parameters in this application, and they are grinding speed dependent. The calibrated model for different mill speeds is suitable for mill speeds lower than 400 r/min. The model is able to simulate the kinetic energy and frictional power losses of the ball assembly of the mill. The simulations revealed that both the kinetic energy and friction power losses had a power relationship with the grinding speed. Further experiments and research are required to evaluate the applicability of the results for a different set of experimental conditions.

Acknowledgements

The research was supported by Natural Sciences and Engineering Research Council of Canada (NSERC) and Mathematics of Information Technology and Complex Systems, Canada (MITACS).

References

Abdellaoui, M., and E. Gaffet.1995. The physics of mechanical alloying in a planetary ball mill: mathematical treatment.*ActaMetallurgicaetMaterialia*, 43(3):1087-1098.

Asaf, Z., D. Rubinstein, and I. Shmulevich.2007. Determination of discrete element model parameters required for soil tillage.*Soil & Tillage Research*, 92(2): 227–242.

Baker, M.L., Y. Chen, C. Lague, H. Landry, Q. Peng, W. Zhong, and J. Wang. 2010. Hemp fibre decortications using a planetary ball mill. *Canadian Biosystems Engineering*, 52(2):2.7-2.15.

Chang, C. S., C. L. Liao, and Q. Shi.2003. Elastic granular materials modeled as first order strain gradient continua. *International Journal of Solids and Structures*, 40: 5565–5582.

Cleary P., and D. Hoyer. 2000. Centrifugal mill charge motion and power draw: comparison of DEM predictions with experiment. *International Journal of Mineral Processing*, 59:131-148.

Cundall, P. A., and O. D. L. Strack.1982. Modeling of microscopic mechanics in granular material. In: J. T. Jenkins, & M. Satake (Eds.), *Mechanics of Granular Materials*: New Models and Constitutive Relations (pp. 113–149). Amsterdam: Elsevier.

Dietz, J. 1999. Hemp growing pains. *The Furrow*,104:16-18.

Fossen, H.2010. Structural Geology. 1st ed. New York, USA: Cambridge University Press.

Fürll, C., and H. Hempel.2000. Effective processing of bastfiber plants and mechanical properties of the fibers. ASABE Paper No. 046091. St. Joseph, Mich.: ASABE.

Gratton, J. L., and Y. Chen.2004. Development of a field-going unit to separate fibre from hemp (Cannabis sativa) stalk. *Applied Engineering in Agriculture*, 20(2):139-145.

Hobson, R. N., D. G. Hepworth, and D. M. Bruce.2001. Quality of fibre separated from unretted hemp stems by decortication.*Journal of Agricultural Engineering Research*, 78(2): 153-158.

Iasonna, A., and M. Magini.1996. Power measurements during mechanical milling. An experimental way to investigate the energy transfer phenomena. *ActaMetallurgicaetMaterialia*, 44(3):1109-1117.

Itasca.2012.Particle Flow Code in 3 Dimensions (PFC^{3D}), Theory and Background. Minneapolis, Minnesota, USA: Itasca consulting group, Inc.

Khan, M. R., Y. Chen, O. Wang, and J. Raghavan.2009. Fineness of hemp (Cannabis Sativa L.) fiber bundle after post-decortication processing using a planetary ball mill. *Applied Engineering in Agriculture*, 25(6):827-834.

Lynch, A., and R. Chester. 2005. The History of grinding. Littleton, Colorado, USA: Society for Mining, Metallurgy and Exploration Inc.

Magini, M., A. Iasonna, and F. Padella.1996. Ball milling: an experimental support to the energy transfer evaluated by the collision model. *ScriptaMaterialia*, 34(1):13-19.

McDowell, G.R., and O. Harireche.2002. Discrete element modelling of yielding and normal compression of sand. *Geotechnique*, 52(4): 299–304.

Mishra, B. K. 2003a. A review of computer simulation of tumbling mills by the discrete element method: part I—contact mechanics. *International Journal of Mineral Processing*, 71:73-93.

Mishra, B. K. 2003b. A review of computer simulation of tumbling mills by the discrete element method: part II - practical applications. *International Journal of Mineral Processing*,71:95-112.

Prasad, B. M., M. M. Sain, and D. N. Roy. 2005. Properties of ball milled thermally treated hemp fibers in an inert atmosphere for potential composite reinforcement. *Journal of Material Science*, 40(16):4271-4278.

Radziszewski, P. 2002. Exploring total media wear. *Mineral Engineering*, 15: 1073-1087.

Rosenkranz, S., S. Breitung-Faes, and A. Kwade.2011. Experimental investigations and modelling of the ball motion in planetary ball mills.*Powder Technology*, 212:224-230.

Sato, A., J. Kano, and F. Saito. 2010. Analysis of abrasion mechanism of grinding media in a planetary mill with DEM simulation. *Advanced Powder Technology*, 21:212-216.

Wills, B. A. 1979. Mineral processing technology: an Introduction to the practical aspects of ore treatment and mineral recovery. 1st ed. Willowdale, Ontario: Pergamon Press.